Nanoscale

COMMUNICATION

View Article Online
View Journal | View Issue

Reversible formation of Ag_{44} from selenolates†

Indranath Chakraborty and T. Pradeep*

Cite this: *Nanoscale*, 2014, **6**, 14190

Received 13th June 2014,
Accepted 3rd October 2014

DOI: 10.1039/c4nr03267e

www.rsc.org/nanoscale

The cluster $Ag_{44}SePh_{30}$, originally prepared from silver selenolate, upon oxidative decomposition by H_2O_2 gives the same cluster back, in an apparently reversible synthesis. Such an unusual phenomenon was not seen for the corresponding thiolate analogues. From several characterization studies such as mass spectrometry, Raman spectroscopy, *etc.*, it has been confirmed that the degraded and as-synthesized selenolates are the same in nature, which leads to the reversible process. The possibility of making clusters from the degraded material makes cluster synthesis economical. This observation makes one to consider cluster synthesis to be a reversible chemical process, at least for selenolates.

Synthesis and characterisation of noble metal quantum clusters is becoming one of the most fascinating topics of materials research due to their unique size-dependent properties.[1–5] Ultra small size and enhanced optical properties make them widely applicable in a variety of applications such as surface enhanced Raman scattering (SERS),[6] catalysis,[7] biolabelling,[8,9] sensing[10,11] and many others.[12–14]

Starting from the Brust protocol,[15] several synthetic routes such as modified Brust synthesis,[16,17] high temperature route,[18] solid state route,[19–22] interfacial synthesis,[23] *etc.* have been developed to create such atomically precise pieces of matter. As of now, most of the reports are on gold clusters and crystal structures of Au_{23},[24] Au_{24},[25] Au_{25},[5,26] Au_{28},[27] Au_{30},[28] Au_{36},[29] Au_{38},[30,31] and Au_{102}.[32] Compared to gold, very few reports exist for silver clusters[33,34] with detailed characterization, which include $Ag_{7,8}$,[23] Ag_9,[20] Ag_{32},[35] Ag_{44}[36] and Ag_{152}.[19] Crystal structures of mixed ligand protected Ag_{14},[37] Ag_{16}[38] and Ag_{32}[38] clusters have been solved. Recently, the crystal structure of the very first complete thiolate protected Ag_{44} cluster has been reported by Bigioni[39] and Zheng[40] groups. The $Ag_{44}(SR)_{30}$ cluster forms a Keplerate solid of concentric icosahedral and dodecahedral atom shells to form a hollow cage which is further protected by six $Ag_2(SR)_5$ units in an octahedral geometry. A similar structure has been proposed for the selenolate analogue of the Ag_{44} cluster[41] which shows an identical optical spectrum with a shift, as expected from the difference in ligands. In most of the cases, the clusters have been examined in terms of their stability.[42–44] As silver clusters are easily oxidisable under aerobic conditions, they degrade rapidly to form thiolates or selenolates and studies on intact clusters are limited.

In this work, we report the reversible formation of the Ag_{44} cluster from selenolates. The reversibility has been checked for other corresponding clusters also but interestingly, except for selenolated Ag_{44}, no other systems (including thiolated Ag_{44}, which is chemically most similar) show this property. The clusters examined include, $Ag_{44}(SPh)_{30}$, $Ag_{44}(4\text{-FTP})_{30}$, and $Ag_{44}(3\text{-FTP})_{30}$, where SPh, 4-FTP and 3-FTP correspond to the thiolate forms of thiophenol, 4-flurothiophenol and 3-flurothiophenol, respectively. A larger silver cluster, $Ag_{152}(PET)_{60}$, was also studied. To explore this phenomenon in more detail, we have oxidised the cluster using peroxide to form selenolates and then the reversibility was checked using borohydride reduction. Several other characterisation studies were done to understand the reversibility.

A two phase solution state route as described in our previous report[41] has been used to synthesize the cluster. Initially, silver trifluoroacetate (0.0714 mmol) was dissolved in 7.2 mL acetonitrile and stirred for 5 min. Benzeneselenol (0.0471 mmol) was added to that solution and was left to stir for another 15 min (resulting in solution A). In another conical flask, 28.6 mL acetonitrile solution of $NaBH_4$ (0.286 mmol) was kept for stirring for 30 min (solution B). Then, solution B was added to solution A and the reaction mixture was left to stir for 3 h at room temperature. A wine red colored cluster was formed after 3 h and it was stored in a refrigerator at ~4 °C.

DST Unit of Nanoscience (DST UNS) and Thematic Unit of Excellence (TUE), Department of Chemistry, Indian Institute of Technology Madras, Chennai 600 036, India. E-mail: pradeep@iitm.ac.in; Fax: +91-44-22570545

†Electronic supplementary information (ESI) available: Details of experimental procedures; instrumentation; reversible cycles, UV/Vis spectra of thiophenol, 4-FTP, 3-FTP protected Ag_{44}, and Ag_{152} cluster; UV/Vis, SEM images and Raman spectra of as-synthesized and degraded thiolates & selenolates; SEM/EDAX of degraded selenolates, UV/Vis of the $Ag_{44}(SePh)_{30}$ cluster under different selenol concentrations and temperatures. See DOI: 10.1039/c4nr03267e

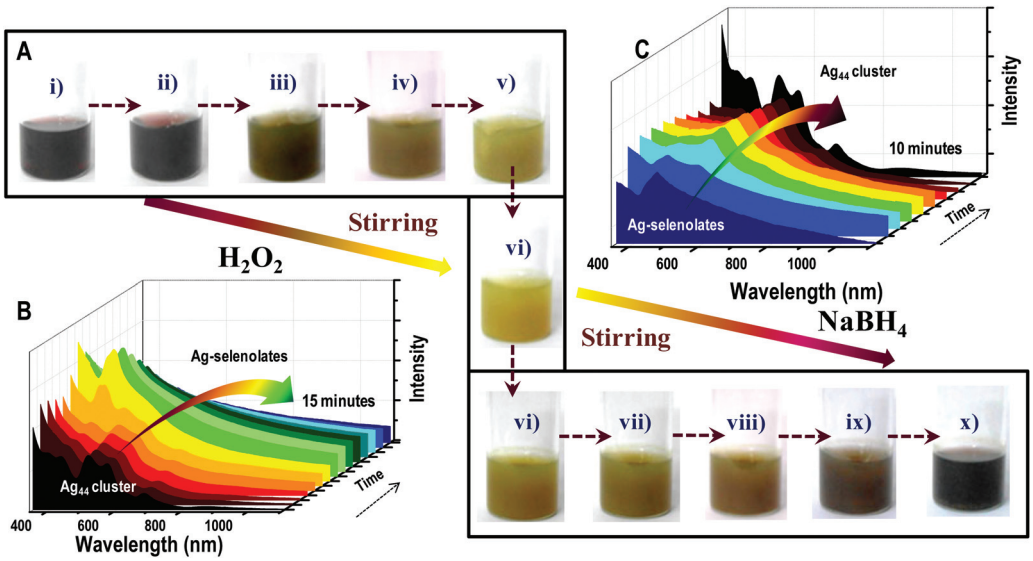

Fig. 1 A: Photographs of the $Ag_{44}(SePh)_{30}$ cluster solution showing time dependent changes during oxidation (i to vi) and reduction (vi to x). Oxidation was accomplished by H_2O_2 and reduction was by $NaBH_4$. B: Time dependent UV/Vis spectra during oxidation of the Ag_{44} cluster to form selenolates. C: Time dependent UV/Vis spectra for the reduction of selenolates to form the Ag_{44} cluster. Each spectrum has been collected at 1 min interval.

Similar methodologies have been followed for thiol protected clusters also. More details are given in the ESI.†

The $Ag_{44}(SePh)_{30}$ cluster[41] shows five intense bands at 1.41 (879), 1.82 (681), 2.16 (574), 2.40 (516) and 2.82 (440) eV (nm) along with three broad bands centered around 1.27 (970), 1.95 (635) and 3.14 (395) eV (nm) in its absorption spectrum. The cluster kept under aerobic conditions will lose its optical identity gradually and a yellow precipitate appears. Reversible cluster formation was observed first from the degraded cluster. Upon addition of adequate amount of borohydride and constant stirring, we observed that the degraded selenolate, formed from the cluster (selenolate **1**) can be reformed to the Ag_{44} cluster in 15 minutes. However, degradation under aerobic conditions typically takes 5–7 days and time dependent observation was difficult. So, an external oxidizing agent, hydrogen peroxide, was added to a controlled amount so that we can monitor oxidation in real time. Photographs at different stages of the reaction are given in Fig. 1A. The cluster is wine red in color but upon addition of H_2O_2, the color changes to yellowish-brown and finally to yellow which confirms the formation of silver selenolate. The reaction was monitored through absorption spectroscopy where the distinct features of the $Ag_{44}(SePh)_{30}$ cluster are lost and subsequently a new peak around 450 nm along with a hump at 430 nm started appearing, due to selenolate. As time progresses, the baseline of the spectrum started increasing because of the low solubility of selenolate in acetonitrile. During the reduction of this selenolate **1** with $NaBH_4$, the color changes in the reverse order and finally the solution becomes clear and attains wine red color which confirms the formation of the Ag_{44} cluster. The corresponding UV/Vis spectra are given in Fig. 1C where the spectra also change in the reverse order. The sharp selenolate peak disappears and all the features of Ag_{44} started appearing with time. The reaction time is controlled by the concentration of the cluster, the amount of H_2O_2 and $NaBH_4$. Constant stirring is also important for this case. For more clarity, these reversible cycles are shown by selecting the intensity of the 516 nm peak for five consecutive cycles (Fig. S1, ESI†).

Similar experiments have been tried for $Ag_{44}(SPh)_{30}$ which is the thiol analogue of $Ag_{44}(SePh)_{30}$. For this cluster, upon addition of H_2O_2 (all concentrations were kept constant) thiolates were formed, as expected. The UV/Vis spectra (Fig. S2A, ESI†) clearly show a sharp peak near 350 nm corresponding to thiolates and the features of the $Ag_{44}(SPh)_{30}$ cluster have been lost completely. Reduction of this degraded thiolate (*thiolate **1***) has resulted in a broad hump near 400 nm and the cluster feature did not develop suggesting that the system was not reversible. We have studied $Ag_{44}(4\text{-FTP})_{30}$ (Fig. S2B, ESI†) and $Ag_{44}(3\text{-FTP})_{30}$ (Fig. S2C, ESI†) also but they both do not show the reversible formation. The '$Ag_{44}(4\text{-FTP})_{30}$ derived thiolate' form nanoparticles by reduction. The plasmonic feature can be seen in the optical spectrum (Fig. S2B, ESI†) while a hump at 480 nm can be observed in the case of '$Ag_{44}(3\text{-FTP})_{30}$-derived thiolate' under the same conditions. Degradation to thiolate is not reversible in the larger cluster, $Ag_{152}(PET)_{60}$ (Fig. S3, ESI†). In the cluster literature, the only case of reversibility was observed by Anand *et al.*[45] who reported that the reversible transformation of human serum albumin protected Ag_9 to the Ag_{14} cluster. Note that the cluster core changes during this transformation. Therefore, the reversibility seen in the case of $Ag_{44}(SePh)_{30}$ is unprecedented. As Au clusters are chemically different in most of their properties,[46] a similar study was not attempted on them.

To find the reason for this unique transformation, a detailed characterization of selenolate **1** was performed.

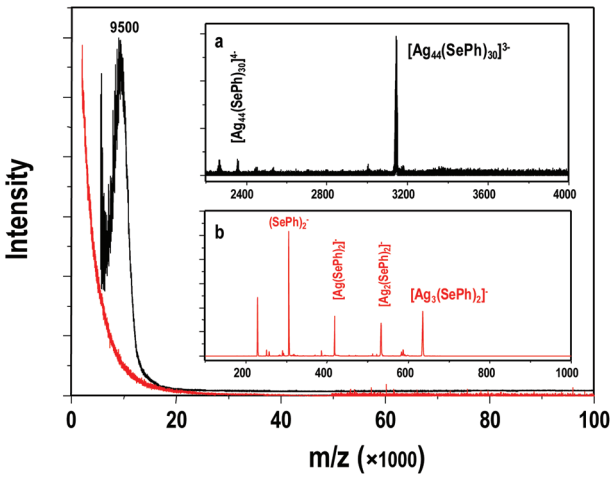

Fig. 2 MALDI MS data of the $Ag_{44}(SePh)_{30}$ cluster (black trace) and selenolate **1** (red trace). Inset shows the ESI mass spectra of the Ag_{44} cluster (a) and selenolate **1** (b), respectively. All the peaks are marked.

Initially, matrix assisted laser desorption ionization mass spectrometry (MALDI MS) was performed for the cluster as well as for selenolate **1** (Fig. 2). $Ag_{44}(SePh)_{30}$ shows a peak centered around *m*/*z* 9500 using DCTB as the matrix[19,33,34] and as expected, selenolate **1** does not show any feature. Electrospray ionization mass spectrometry (ESI MS) shows 3, 4 features (Fig. 2a) of $Ag_{44}(SePh)_{30}$ which confirm the purity of the cluster. As selenolates have very less solubility, a methanol–acetonitrile mixture was used for the ESI measurement. Some selenolate species such as $Ag_3(SePh)_2$, $Ag_2(SePh)_2$ and $Ag(SePh)_2$ have been observed in the negative ion mode. For confirmation, ESI-MS was also taken for the reversibly formed Ag_{44} cluster which shows the same feature as depicted in Fig. 2A.

We thought that comparison of selenolate **1** with the as-synthesized selenolate (selenolate **2**) and similar thiolate samples (synthesis procedures are given in ESI†) might be useful to understand this phenomenon. UV/Vis spectroscopy for both the cases have been compared (Fig. S4, ESI†) and it was found that for the case of selenolate, the spectra are comparable (Fig. S4A, ESI†) but drastic differences are seen for thiolates (Fig. S4B, ESI†). As-synthesized thiolate (*thiolate 2*) shows a sharp peak at 237 nm and a broad hump at 277 nm whereas thiolate **1** shows four broad humps at 240, 280, 360 and 420 nm, respectively. Selenolate **1** shows a peak at 464 nm along with a hump at 430 nm and similar two peaks at 430 and 450 nm were observed for selenolate **2**. So, selenolates **1** and **2** might be the same as it appears in absorption spectroscopy. To understand it better, laser desorption ionization mass spectrometric (LDI MS) analysis was attempted for the thiolates and selenolates (Fig. 3). It is important to mention here that LDI MS has been used as these thiolates and selenolates have very less solubility, so it was difficult to perform electrospray ionization (ESI) or matrix assisted laser desorption ionization (MALDI) mass analysis. Here also similar trends have been observed in absorption spectroscopy. Systematic Ag_2S losses have been observed for both the thiolates (Fig. 3A) but the loss started from higher mass (*m*/*z* 4500) for thiolate **2** while it started from *m*/*z* 1800 for thiolate **1**, that too with much lower intensity (an expanded view of a peak at *m*/*z* 1375 is shown in the inset of Fig. 3A). Interestingly, in the lower mass, intensity gradually increases for thiolate **2** and some shifts have also been observed. The data suggest that thiolates **1** and **2** are different in nature. Selenolates show similar features and systematic Ag_2Se losses have been seen (Fig. 3B) from almost the same mass region and the isotope pattern is also similar (inset of Fig. 3B). The reason for the complicated fine structure of selenolates compared to thiolates is because of the isotopes of Se. Selenium has six isotopes namely, ^{74}Se (0.89%), ^{76}Se (9.37%), ^{77}Se (7.63%), ^{78}Se (23.77%), ^{80}Se (49.61%), and ^{82}Se (8.73%), which contribute significantly to the fine mass spectral features compared to sulfur which has only one predominant isotope, namely ^{32}S (95%). Raman spectroscopy was used to confirm that selenolates are the same but thiolates are different in nature (Fig. S5, ESI†). Although detailed peak assignments have not been done, many are assigned based on the literature.[47] From a comparative study, we can see that Raman features for selenolates **1** and **2** (Fig. S5A, ESI†) are the same but differences are there for thiolates (Fig. S5, ESI†). The peak at 1070 cm^{-1} (ring deformation mode[47]) for thiolate **1** has been split for thiolate **2** along with some more additional peaks near 1020 cm^{-1} (ring breathing mode[47]). Differences were observed for thiolates in SEM images (Fig. S6, ESI†). As-synthesized thiolates appear amorphous whereas degraded ones show crystalline nature. For the case of selenolates, both show porous structures (Fig. S6, ESI†). From the SEM/EDAX analysis, the ratio of Ag : Se for the degraded selenolate species is found to be 1 : 0.68 (3 : 2.04) which is very close to the atomic ratios present in the cluster (Fig. S7, ESI†). Non-stoichiometry in thiolates was found earlier[48–51] and a similar case is expected for selenolates also. Parikh *et al.* have shown the existence of silver rich thiolates

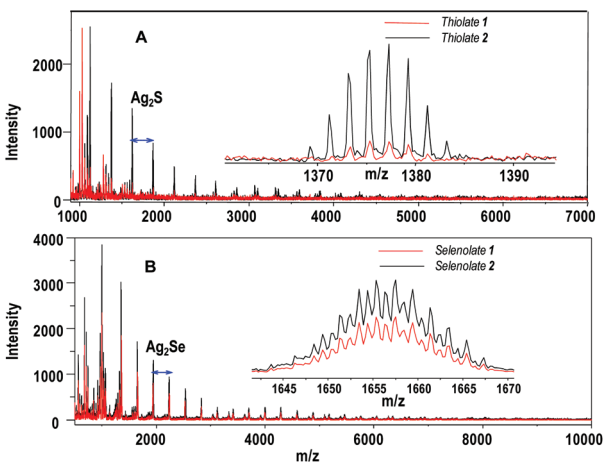

Fig. 3 Comparative LDI mass spectra of thiolates (A) and selenolates (B). Insets for both the cases show an extended view of some selected peaks centred at *m*/*z* 1377 (for thiolates) and *m*/*z* 1656 (for selenolates). True ion intensities are compared and not relative abundances.

using elemental analysis.[52] Li *et al.*[48,49] and Sun *et al.*[50] have shown the crystal structures of metal rich thiolates. McLauchlan and Ibers have shown sulphur and selenium rich silver thiolates.[53] So it is not difficult to rationalize the existence of non-stoichiometric thiolates or selenolates in our experiments. In detail such thiolates may be structures with sulphide cores with thiolate shells, although the authors refer to them as thiolates.

From all these data it is confirmed that degraded and as-synthesized selenolates are the same in nature and because of that formation of $Ag_{44}SePh_{30}$ is reversible. Another reason for the reversibility could be the higher stability of this selenolate protected Ag_{44} cluster compared to the thiol protected one. To confirm this, the cluster has been synthesized with different concentrations of benzeneselenol and surprisingly, all of them resulted in Ag_{44} clusters with distinct optical and mass spectral features (Fig. S8, ESI†). The cluster has been synthesized at different temperatures and surprisingly, in all the cases (from 0 to 60 °C) they formed (Fig. S9, ESI†) which suggests the high stability of the system. Formation time of the cluster reduced drastically with increase in temperature, which is expected (inset of Fig. S9, ESI†). For the thiol case, irreversibility has been observed because of the different nature of the thiolates and may be upon reduction, thiolates have many possibilities to make diverse clusters or bigger nanoparticles.

In summary, we have synthesized selenolate and thiolate analogues of Ag_{44} clusters using similar synthetic methodologies. Unusual reversible formation of the Ag_{44} cluster from selenolate was observed. This phenomenon has not been seen for the corresponding thiolates. Several characterization techniques have been used to understand the reversibility. It has been found that degraded selenolates and as-synthesized selenolates are the same in nature but they are different in the case of thiolates, which is responsible for this unusual property. This opens up a new possibility of making clusters from the degraded materials, which may be economical for precious metals like gold and silver. The most important aspect of this finding appears to be that cluster synthesis is proven to be reversible, at least in the limited case of selenolates. This suggests that clusters may be treated just as molecules in their chemistry.

We thank the Department of Science and Technology, Government of India for constantly supporting our research program on nanomaterials. I. C. thanks IITM for research fellowships.

Notes and references

1 C. M. Aikens, *J. Phys. Chem. C*, 2008, **112**, 19797–19800.
2 T. P. Bigioni, R. L. Whetten and Ö. Dag, *J. Phys. Chem. B*, 2000, **104**, 6983–6986.
3 S. Link, A. Beeby, S. FitzGerald, M. A. El-Sayed, T. G. Schaaff and R. L. Whetten, *J. Phys. Chem. B*, 2002, **106**, 3410–3415.
4 K. Nobusada and T. Iwasa, *J. Phys. Chem. C*, 2007, **111**, 14279–14282.
5 M. Zhu, C. M. Aikens, F. J. Hollander, G. C. Schatz and R. Jin, *J. Am. Chem. Soc.*, 2008, **130**, 5883–5885.
6 I. Chakraborty, S. Bag, U. Landman and T. Pradeep, *J. Phys. Chem. Lett.*, 2013, **4**, 2769–2773.
7 S. Yamazoe, K. Koyasu and T. Tsukuda, *Acc. Chem. Res.*, 2014, **47**, 816–824.
8 C.-A. J. Lin, T.-Y. Yang, C.-H. Lee, S. H. Huang, R. A. Sperling, M. Zanella, J. K. Li, J.-L. Shen, H.-H. Wang, H.-I. Yeh, W. J. Parak and W. H. Chang, *ACS Nano*, 2009, **3**, 395–401.
9 M. A. H. Muhammed and T. Pradeep, in *Advanced Fluorescence Reporters in Chemistry and Biology II*, ed. A. P. Demchenko, Springer, Berlin Heidelberg, 2010, vol. 9, ch. 11, pp. 333–353.
10 I. Chakraborty, T. Udayabhaskararao and T. Pradeep, *J. Hazard. Mater.*, 2012, **211–212**, 396–403.
11 A. Mathew, P. R. Sajanlal and T. Pradeep, *Angew. Chem., Int. Ed.*, 2012, **51**, 9596–9600.
12 I. Chakraborty, T. Udayabhaskararao, G. K. Deepesh and T. Pradeep, *J. Mater. Chem. B*, 2013, **1**, 4059–4064.
13 T. Chen, S. Xu, T. Zhao, L. Zhu, D. Wei, Y. Li, H. Zhang and C. Zhao, *ACS Appl. Mater. Interfaces*, 2012, **4**, 5766–5774.
14 Y. Kong, J. Chen, F. Gao, R. Brydson, B. Johnson, G. Heath, Y. Zhang, L. Wu and D. Zhou, *Nanoscale*, 2013, **5**, 1009–1017.
15 M. Brust, M. Walker, D. Bethell, D. J. Schiffrin and R. Whyman, *J. Chem. Soc., Chem. Commun.*, 1994, 801–802.
16 S. Gaur, J. T. Miller, D. Stellwagen, A. Sanampudi, C. S. S. R. Kumar and J. J. Spivey, *Phys. Chem. Chem. Phys.*, 2012, **14**, 1627–1634.
17 J. Kim, K. Lema, M. Ukaigwe and D. Lee, *Langmuir*, 2007, **23**, 7853–7858.
18 I. Chakraborty, T. Udayabhaskararao and T. Pradeep, *Chem. Commun.*, 2012, **48**, 6788–6790.
19 I. Chakraborty, A. Govindarajan, J. Erusappan, A. Ghosh, T. Pradeep, B. Yoon, R. L. Whetten and U. Landman, *Nano Lett.*, 2012, **12**, 5861–5866.
20 T. U. B. Rao, B. Nataraju and T. Pradeep, *J. Am. Chem. Soc.*, 2010, **132**, 16304–16307.
21 I. Chakraborty, R. G. Bhuin, S. Bhat and T. Pradeep, *Nanoscale*, 2014, **6**, 8561–8564.
22 A. Ganguly, I. Chakraborty, T. Udayabhaskararao and T. Pradeep, *J. Nanopart. Res.*, 2013, **15**, 1–7.
23 T. Udaya Bhaskara Rao and T. Pradeep, *Angew. Chem., Int. Ed.*, 2010, **49**, 3925–3929.
24 A. Das, T. Li, K. Nobusada, C. Zeng, N. L. Rosi and R. Jin, *J. Am. Chem. Soc.*, 2013, **135**, 18264–18267.
25 A. Das, T. Li, K. Nobusada, Q. Zeng, N. L. Rosi and R. Jin, *J. Am. Chem. Soc.*, 2012, **134**, 20286–20289.
26 M. W. Heaven, A. Dass, P. S. White, K. M. Holt and R. W. Murray, *J. Am. Chem. Soc.*, 2008, **130**, 3754–3755.
27 C. Zeng, T. Li, A. Das, N. L. Rosi and R. Jin, *J. Am. Chem. Soc.*, 2013, **135**, 10011–10013.
28 D. Crasto, S. Malola, G. Brosofsky, A. Dass and H. Häkkinen, *J. Am. Chem. Soc.*, 2014, **136**, 5000–5005.

29 C. Zeng, H. Qian, T. Li, G. Li, N. L. Rosi, B. Yoon, R. N. Barnett, R. L. Whetten, U. Landman and R. Jin, *Angew. Chem., Int. Ed.*, 2012, **51**, 13114–13118.
30 Y. Pei, Y. Gao and X. C. Zeng, *J. Am. Chem. Soc.*, 2008, **130**, 7830–7832.
31 H. Qian, W. T. Eckenhoff, Y. Zhu, T. Pintauer and R. Jin, *J. Am. Chem. Soc.*, 2010, **132**, 8280–8281.
32 P. D. Jadzinsky, G. Calero, C. J. Ackerson, D. A. Bushnell and R. D. Kornberg, *Science*, 2007, **318**, 430–433.
33 I. Chakraborty, J. Erusappan, A. Govindarajan, K. Sugi, T. Udayabhaskararao, A. Ghosh and T. Pradeep, *Nanoscale*, 2014, **6**, 8024–8031.
34 K. S. Sugi, I. Chakraborty, T. Udayabhaskararao, J. S. Mohanty and T. Pradeep, *Part. Part. Syst. Charact.*, 2013, **30**, 241–243.
35 J. Guo, S. Kumar, M. Bolan, A. Desireddy, T. P. Bigioni and W. P. Griffith, *Anal. Chem.*, 2012, **84**, 5304–5308.
36 K. M. Harkness, Y. Tang, A. Dass, J. Pan, N. Kothalawala, V. J. Reddy, D. E. Cliffel, B. Demeler, F. Stellacci, O. M. Bakr and J. A. McLean, *Nanoscale*, 2012, **4**, 4269–4274.
37 H. Yang, J. Lei, B. Wu, Y. Wang, M. Zhou, A. Xia, L. Zheng and N. Zheng, *Chem. Commun.*, 2013, **49**, 300–302.
38 H. Yang, Y. Wang and N. Zheng, *Nanoscale*, 2013, **5**, 2674–2677.
39 A. Desireddy, B. E. Conn, J. Guo, B. Yoon, R. N. Barnett, B. M. Monahan, K. Kirschbaum, W. P. Griffith, R. L. Whetten, U. Landman and T. P. Bigioni, *Nature*, 2013, **501**, 399–402.
40 H. Yang, Y. Wang, H. Huang, L. Gell, L. Lehtovaara, S. Malola, H. Häkkinen and N. Zheng, *Nat. Commun.*, 2013, 4.
41 I. Chakraborty, W. Kurashige, K. Kanehira, L. Gell, H. Häkkinen, Y. Negishi and T. Pradeep, *J. Phys. Chem. Lett.*, 2013, **4**, 3351–3355.
42 A. Desireddy, S. Kumar, J. Guo, M. D. Bolan, W. P. Griffith and T. P. Bigioni, *Nanoscale*, 2013, **5**, 2036–2044.
43 A. C. Dharmaratne, T. Krick and A. Dass, *J. Am. Chem. Soc.*, 2009, **131**, 13604–13605.
44 T. G. Schaaff and R. L. Whetten, *J. Phys. Chem. B*, 1999, **103**, 9394–9396.
45 U. Anand, S. Ghosh and S. Mukherjee, *J. Phys. Chem. Lett.*, 2012, **3**, 3605–3609.
46 A. Mathew and T. Pradeep, *Part. Part. Syst. Charact.*, 2014, DOI: 10.1002/ppsc.201400033.
47 S. K. Saikin, R. Olivares-Amaya, D. Rappoport, M. Stopa and A. Aspuru-Guzik, *Phys. Chem. Chem. Phys.*, 2009, **11**, 9401–9411.
48 B. Li, R.-W. Huang, J.-H. Qin, S.-Q. Zang, G.-G. Gao, H.-W. Hou and T. C. W. Mak, *Chem. – Eur. J.*, 2014, **20**, 12416–12420.
49 G. Li, Z. Lei and Q.-M. Wang, *J. Am. Chem. Soc.*, 2010, **132**, 17678–17679.
50 D. Sun, H. Wang, H.-F. Lu, S.-Y. Feng, Z.-W. Zhang, G.-X. Sun and D.-F. Sun, *Dalton Trans.*, 2013, **42**, 6281–6284.
51 I. Casals, P. González-Duarte, J. Sola, J. Vives, M. Font-Bardia and X. Solans, *Polyhedron*, 1990, **9**, 769–771.
52 A. N. Parikh, S. D. Gillmor, J. D. Beers, K. M. Beardmore, R. W. Cutts and B. I. Swanson, *J. Phys. Chem. B*, 1999, **103**, 2850–2861.
53 C. C. McLauchlan and J. A. Ibers, *Inorg. Chem.*, 2001, **40**, 1809–1815.